

Unsupervised deep learning-based anomaly detection in mixed gases using sensor array

Dang Thi Thu Ha^{1,2,3*}, Nguyen Dinh Van², Nguyen Duc Hoa³

¹Hoalu University, Xuan Thanh, Hoa Lu, Ninh Binh, Viet Nam;

²School of Electrical and Electronic Engineering, Hanoi University of Science and Technology, 1 Dai Co Viet, Bach Mai, Hanoi, Vietnam;

³School of Materials Science and Engineering, Hanoi University of Science and Technology, 1 Dai Co Viet, Bach Mai, Hanoi, Vietnam.

*Corresponding author: dttha.nnth@hluv.edu.vn

Received 19 Apr. 2026; Revised 8 Jun. 2026; Accepted 15 Jun. 2026; Published 25 Jun. 2026.

DOI: <https://doi.org/10.54939/1859-1043.j.mst.112.2026.141-148>

ABSTRACT

Anomaly detection in mixed-gas data is a significant challenge for multisensor systems because of their nonlinear characteristics, noise, environmental influences, and scarcity of anomalous data. This study proposes an unsupervised deep-learning anomaly detection method. An unsupervised Autoencoder model was employed to reconstruct two-dimensional image representations of normal mixed-gas data, thereby eliminating the need for anomalous labels during training. To simulate realistic abnormal conditions, anomalous samples were generated using diverse and physically meaningful perturbation transformation methods. An adaptive threshold based on the reconstruction error was used as the criterion for distinguishing between normal and anomalous data points. The effectiveness of the proposed method was evaluated using accuracy and F1-score metrics, which achieved values of 0.97 and 0.92, respectively. The experimental results demonstrate that the proposed approach can effectively learn the characteristics of normal data and accurately detect anomalies in mixed gas datasets. This method improves the safety, reliability, and intelligent monitoring capabilities of gas-sensor array systems in practical applications.

Keywords: Anomaly detection; Unsupervised learning; Autoencoder; Gas sensor array.

1. INTRODUCTION

In recent years, gas-sensing systems based on sensor arrays have attracted significant attention owing to their wide range of applications in environmental monitoring, industrial safety, food quality assessment, and biomedical diagnosis. By integrating multiple sensors with different sensitivities, these systems can capture complex response patterns from various gases and gas mixtures, thereby providing more comprehensive information than single-sensor systems [1].

However, under real operating conditions, the performance of these systems is often affected by various factors, such as environmental noise, sensor drift, nonlinear responses, cross-sensitivity among gases, and sensor faults [2]. In addition, abnormal conditions, such as sudden signal fluctuations, severe noise, or out-of-distribution gas samples, may alter the data distribution, leading to degraded accuracy and reliability of the prediction models [3]. Therefore, anomaly detection has become an important task for improving the stability and reliability of intelligent gas-sensing systems.

Traditional anomaly detection methods, such as PCA, one-class SVM, KNN, and DNN, have been widely applied in gas-sensing applications [4]. However, these approaches often rely on labeled abnormal data, whereas abnormal samples in real-world scenarios are rare, difficult to collect, and highly diverse. Furthermore, many abnormal conditions may not appear during the training phase, limiting the generalization capability of supervised learning methods. Consequently, unsupervised learning approaches have emerged as a promising direction because they can learn the intrinsic characteristics of normal data without requiring anomaly labels [5].

Recently, Deep Learning techniques, particularly autoencoders, have demonstrated remarkable effectiveness in unsupervised anomaly detection tasks [6]. Autoencoders can learn the latent representations of normal data and reconstruct them with low reconstruction errors, whereas abnormal samples generally produce larger reconstruction errors. Therefore, the reconstruction error can be effectively used as a criterion to detect abnormal operating conditions.

Motivated by these advantages, this study proposes an unsupervised anomaly detection method for sensor array data based on image representation and a Convolutional Autoencoder model. Specifically, multidimensional sensor signals are transformed into image representations to exploit the spatiotemporal feature learning capabilities of convolutional networks. The Autoencoder is then trained using normal data, and anomalies are detected based on the reconstruction errors combined with an adaptive threshold. In addition, several physically meaningful anomaly types, including sensor noise, signal drift, sudden changes, local disturbances, and sensor faults, were generated to simulate the real operating conditions. The experimental results demonstrate that the proposed method can effectively detect abnormal conditions, thereby improving the stability and reliability of e-nose systems in complex and unstable environments.

2. MATERIALS AND METHODS

2.1. Gas mixture dataset

The dataset used in this study was a publicly available gas sensor dataset obtained from the UCI Machine Learning Repository. This dataset was first collected by Fonollosa et al. [7], and a detailed description is provided in [8].

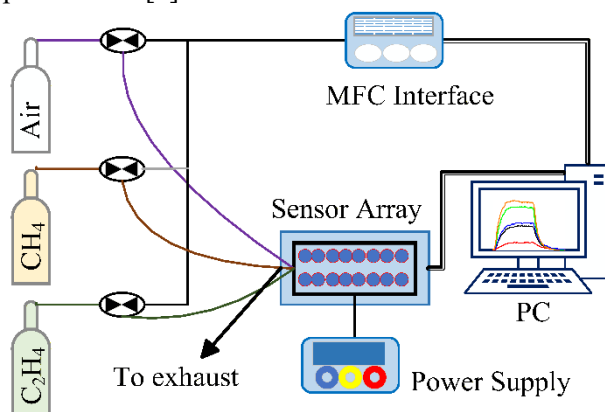


Figure 1. Schematic of the gas mixture measurement system.

The dataset consisted of time-series measurements acquired from an array of 16 chemical sensors manufactured by Figaro, Inc. (USA), including four different sensor types: TGS-2600, TGS-2602, TGS-2610, and TGS-2620, with four sensors of each type. The experimental setup for gas measurements using the multisensor gas array is shown in Figure 1. Clean air, methane (CH_4), and ethylene (C_2H_4) gases were controlled using mass flow controllers (MFCs) and mixed before being injected into the sensor chamber. The sensor responses were continuously acquired and transmitted to a computer for real-time monitoring and data storage, and the exhaust gases were released through an outlet.

During data acquisition, the gas concentrations were not kept constant but dynamically varied over time to simulate realistic environmental conditions, as shown in Figure 2. Specifically, the concentration transitions occurred at random intervals ranging from 80 to 120 s, with the concentration levels also randomly selected. The methane concentrations ranged from 0 to 296.67 ppm, and the ethylene concentrations varied from 0 to 20 ppm. The dataset contained 4,178,504 samples of methane–ethylene gas mixtures.

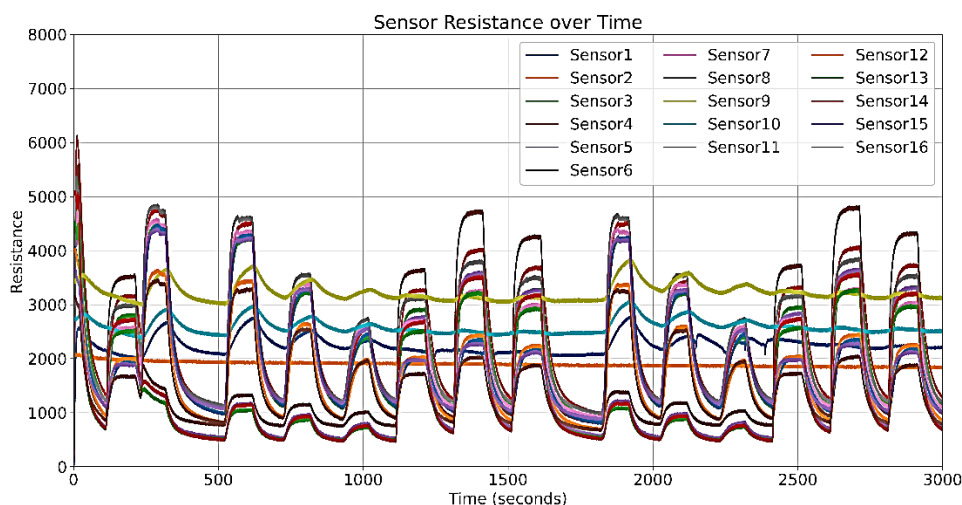


Figure 2. Sensor resistance response to methane–ethylene gas mixtures.

2.2. Gas sensor array data converted into 2D grayscale images

The input data consisted of time-series signals acquired from a gas sensor array, where each sample represented the collective response of all the sensors at a specific time under a particular gas mixture condition. The sensor values were first normalized to the range of [0, 1] and then linearly interpolated along the vertical axis to obtain a uniform width of 128 columns, thereby ensuring consistent image dimensions across all the samples. Subsequently, the normalized values were converted to an 8-bit grayscale (0–255) scale.

Each sensor column was replicated four times ($16 \times 4 = 64$), and each temporal row was duplicated twice ($64 \times 2 = 128$). To simultaneously exploit the spatial correlations among the sensor channels and the temporal dynamics of the signals, each sequence was transformed into a two-dimensional grayscale image with a fixed resolution of 128×128 . In the resulting image, the vertical axis corresponds to the sensor indices, and the horizontal axis represents the temporal evolution of the signal, as illustrated in Figure 3.

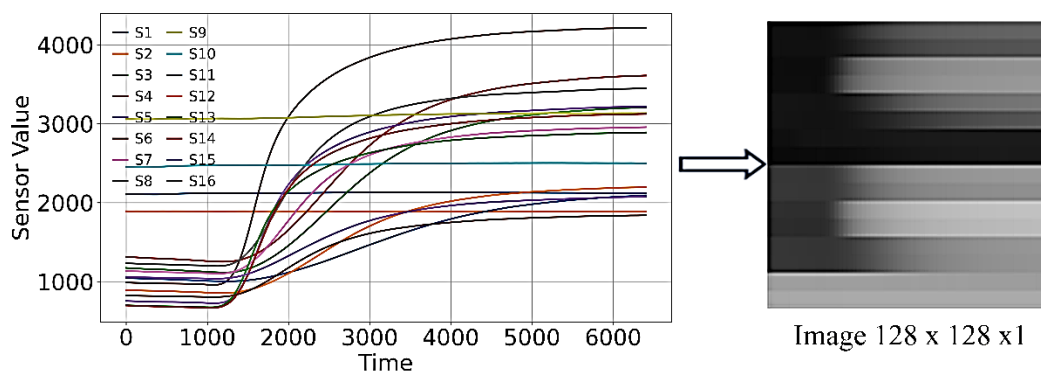


Figure 3. Conversion of array sensor data into grayscale images.

To increase the dataset size and improve the generalization capability of the model, a sliding-window technique with a window length of 6400 samples and a stride of 5 samples for each gas mixture was applied, resulting in a five-fold data augmentation factor [9]. After completing the preprocessing, data augmentation, and image transformation stages, the mixed-gas dataset consisted of 1,625 normal methane–ethylene mixture images. 1,625 normal images were divided into five subsets. Four subsets (1,300 images) were used for normal training, and the remaining subset (325 images) was reserved for normal testing.

2.3. Anomaly simulation on the dataset

The anomaly simulation process was designed to be physically and technically meaningful for gas-sensing systems while ensuring diverse anomaly types. Anomalies were defined as data samples that deviated from the distribution of normal data, representing faulty states or undesirable operating conditions of the sensor-array system. The generated anomalies were intended to reflect realistic failure mechanisms in gas-sensing systems, including measurement random noise, sensor drift, random patch, abrupt changes, and sensor fault.

To improve realism, instead of using completely discrete transitions, the proposed approach employs smooth transition regions based on a sigmoid function to preserve the physical continuity of the signals and avoid generating obvious anomalies. In this study, anomalous data were generated using a composite transformation function applied directly to each normal data sample. Specifically, for each input signal image, one or multiple anomaly transformations were randomly selected with varying anomaly severity levels and sequentially applied instead of introducing only a single type of anomaly.

2.4. Network structure

The architecture of the convolutional Autoencoder is presented in Table 1. The encoder compresses the input image into a $4 \times 4 \times 8$ latent representation through four convolutional layers and a max-pooling layer, whereas the decoder reconstructs the image to its original size ($128 \times 128 \times 1$) using upsampling and convolutional operations. ReLU and Sigmoid activation functions were used in the hidden and output layers, respectively, and the network was optimized using the MSE loss function.

Table 1. Autoencoder architecture.

Stage	Layer	Filters	Kernel Size	Stride	Activation	Output Shape
Input	InputLayer	-	-	-	-	$128 \times 128 \times 1$
Encoder	Conv2D	32	5×5	2	ReLU	$64 \times 64 \times 32$
Encoder	Conv2D	16	5×5	2	ReLU	$32 \times 32 \times 16$
Encoder	Conv2D	8	5×5	2	ReLU	$16 \times 16 \times 8$
Encoder	Conv2D	8	5×5	2	ReLU	$8 \times 8 \times 8$
Encoder	MaxPooling2D	-	2×2	2	-	$4 \times 4 \times 8$
Latent space	Flatten	-	-	-	-	128
Decoder	Reshape	-	-	-	-	$4 \times 4 \times 8$
Decoder	UpSampling2D	-	2×2	-	-	$8 \times 8 \times 8$
Decoder	Conv2D	8	5×5	1	ReLU	$8 \times 8 \times 8$
Decoder	UpSampling2D	-	2×2	-	-	$16 \times 16 \times 8$
Decoder	Conv2D	8	5×5	1	ReLU	$16 \times 16 \times 8$
Decoder	UpSampling2D	-	2×2	-	-	$32 \times 32 \times 8$
Decoder	Conv2D	16	5×5	1	ReLU	$32 \times 32 \times 16$
Decoder	UpSampling2D	-	2×2	-	-	$64 \times 64 \times 16$
Decoder	Conv2D	32	5×5	1	ReLU	$64 \times 64 \times 32$
Decoder	UpSampling2D	-	2×2	-	-	$128 \times 128 \times 32$
Output	Conv2D	1	5×5	1	Sigmoid	$128 \times 128 \times 1$

Figure 4 illustrates the anomaly detection framework based on a Deep Convolutional Autoencoder for gas sensor data. First, the time-series signals from the sensor array were

transformed into grayscale images with a resolution of 128×128 pixels. 1,300 images were used for normal training. These images were then fed into the autoencoder network, consisting of an Encoder and a Decoder, to learn the latent feature representations and reconstruct the input images. The reconstruction error between the original and reconstructed images was calculated using the Mean Squared Error (MSE). Finally, an adaptive threshold based on the mean (μ), threshold adjustment coefficient (α), and standard deviation (σ) was applied to classify the samples as normal or anomalous.

The threshold is determined from the normal training samples as (1):

$$\text{Threshold Min} = \mu_{\epsilon} - \alpha\sigma_{\epsilon}, \text{Threshold Max} = \mu_{\epsilon} + \alpha\sigma_{\epsilon} \quad (1)$$

Where: μ_{ϵ} , σ_{ϵ} : mean and standard deviation of reconstruction errors between the original images and the reconstructed images, respectively, α scaling factor.

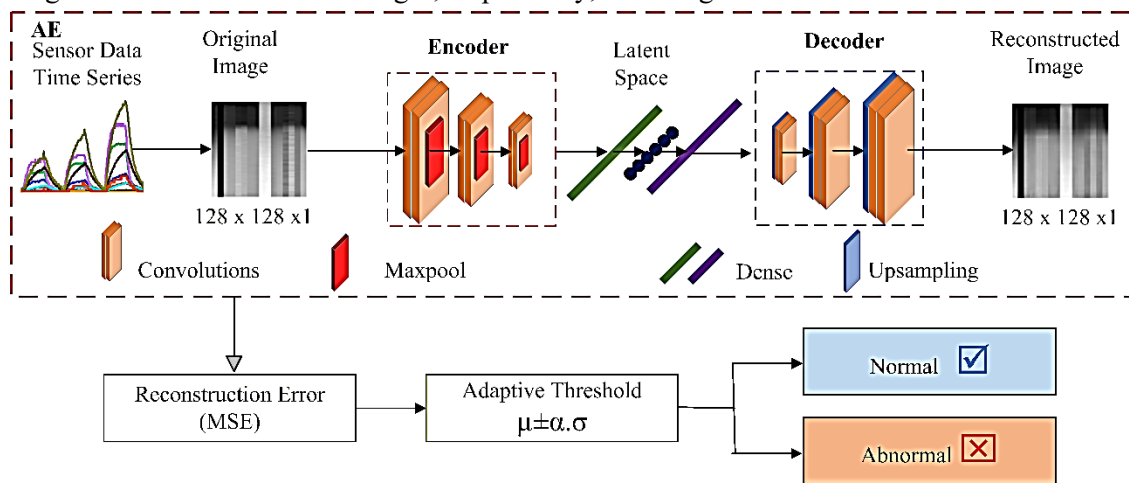


Figure 4. Architecture of the deep convolutional autoencoder for anomaly detection.

3. RESULTS AND DISCUSSION

3.1. Training of the autoencoder model

Figure 5 illustrates the variation in the loss function for the training and validation sets over the training epochs during the autoencoder training process. The model was trained in a stable manner, converged rapidly, and achieved high predictive performance with low loss values that were maintained throughout the training process.

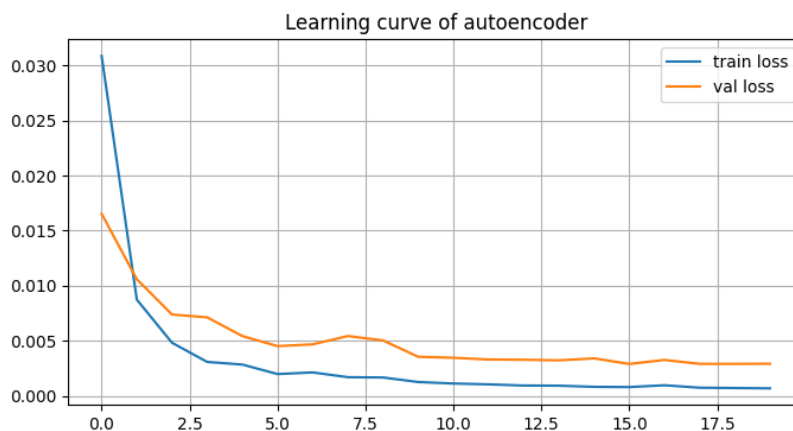


Figure 5. Learning curves of the autoencoder model.

3.2. Mean squared deviation reconstruction error distribution

The Kernel Density Estimation (KDE) and Cumulative Distribution Function (CDF) plots shown in Figure 6 demonstrate that normal samples exhibit low reconstruction errors with concentrated distributions, whereas anomalous samples show significantly larger reconstruction errors with broader distributions. The KDE curves clearly indicate the separation between normal and anomalous data, whereas the CDF curves further confirm that anomalous samples accumulate more slowly because of the higher reconstruction error values. These results demonstrate that the proposed autoencoder model can effectively distinguish between normal and anomalous operating conditions using an adaptive threshold based on the reconstruction errors.

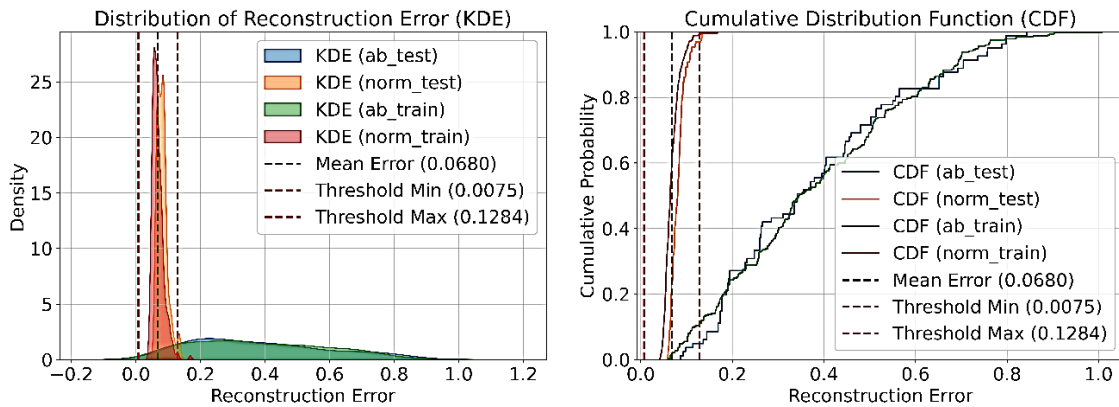


Figure 6. KDE and CDF analyses of the reconstruction errors.

3.3. Anomaly detection using adaptive threshold

The 325 normal testing images were further augmented fivefold using sliding-window shifting, resulting in 1,625 normal testing images. A total of 1,625 normal images were used in the anomaly simulation. To obtain an anomaly ratio of 0.2, 406 abnormal images were generated. The experimental evaluation demonstrated that $\alpha = 2.5$ achieved the best trade-off between Precision and Recall and yielded the highest F1-score among the tested values. The results in Tables 2 and 3 demonstrate that the anomaly detection model achieved high and stable performance. The confusion matrix shows that the model correctly classified 1625 normal samples and 366 abnormal samples, while only 20 false alarms and 40 missed anomalies were observed. These results indicate that the model can effectively distinguish between normal and abnormal data.

In the classification report in Table 3, the normal class achieved a Precision, Recall, and F1-score of 0.98, 0.99, and 0.98, respectively, demonstrating the highly accurate recognition of normal samples. For the Abnormal class, the model obtained a precision of 0.95, recall of 0.90, and F1-score of 0.92, indicating a strong anomaly detection capability despite a few missed abnormal cases. Furthermore, the overall accuracy reached 97% with a Macro F1-score of 0.95, confirming the effectiveness and robustness of the proposed anomaly detection approach.

Table 2. Confusion matrix.

	Pred Normal	Pred Abnormal
True Normal	1605	20
True Abnormal	40	366

The results indicate that the autoencoder model with adaptive thresholds outperforms the machine learning methods, as shown in Table 4.

Table 5 shows that the proposed model achieved the best performance for noise and sensor failure anomalies, both of which obtained perfect recall. Random patches were the most difficult anomaly type to detect, whereas signal drift and abrupt changes achieved moderate detection

performance. Overall, the results indicate that the model is more sensitive to severe signal distortions than to localized anomalies.

Table 3. Classification report.

	Precision	Recall	F1-score	Support
Normal	0.98	0.99	0.98	1625
Abnormal	0.95	0.90	0.92	406
Accuracy			0.97	2031
Macro avg	0.96	0.94	0.95	2031
Weighted avg	0.97	0.97	0.97	2031

Table 4. Performance of anomaly detection models.

Model	Precision	Recall	F1-score
Autoencoder	0.95	0.90	0.92
SVM	0.86	0.83	0.84
Random Forest	0.80	0.78	0.79
MLP	0.76	0.74	0.75

Table 5. Detection performance for different anomaly types.

Anomaly Type	Number of Anomalies	Precision	Recall	F1-score
Random noise	86	1.00	1.00	1.00
Sensor fault	86	0.98	1.00	0.99
Random patch	85	0.85	0.77	0.81
Sensor drift	85	0.90	0.87	0.88
Abrupt change	64	0.86	0.84	0.85

4. CONCLUSIONS

This study proposed an unsupervised autoencoder-based anomaly detection method for mixed-gas data acquired using gas sensor arrays. The proposed approach effectively learns the characteristics of normal data through a signal reconstruction mechanism without requiring anomalous labels during the training process, thereby addressing the challenge of insufficient anomalous data in practical gas sensing systems. In addition, anomalous samples were generated using diverse and physically meaningful perturbation mechanisms to simulate abnormal conditions encountered in real-world environments. The experimental results demonstrated that the proposed method achieved an accuracy of 97% and an F1-score of 0.92, confirming its effectiveness in detecting anomalies in nonlinear and highly noisy mixed-gas data. This study contributes to improving the reliability, safety, and intelligent monitoring capabilities of multi-sensor gas-sensing systems for practical applications. In future work, the proposed approach will be extended to more complex mixed-gas datasets and integrated with advanced deep learning models to further enhance its real-time applicability.

Acknowledgement: This research is funded by Vietnam National Foundation for Science and Technology Development (NAFOSTED) under grant number 103.02-2024.15.

REFERENCES

- [1]. F. Zhang, Z. Zhu, J. Liu, Y. Zhang, M. Xu, and P. Jia, "A Novel Concentration Prediction Technique of Carbon Monoxide (CO) Based on Beluga Whale Optimization-Extreme Gradient Boosting (BWO-XGBoost)", *Journal of the Taiwan Institute of Chemical Engineers*, Vol. 171, p. 106045, (2025).
- [2]. G. Sberveglieri, G. Greco, D. Genzardi, E. Núñez-Carmona, S. Pezzottini, and V. Sberveglieri, "The Electronic Nose: Review on Sensor Arrays and Future Perspectives", *Chemical Engineering Transactions*, Vol. 95, pp. 265–270, (2022).

- [3]. Y. Heng, Y. Zhou, D. H. Nguyen, V. D. Nguyen, and M. Jiao, "An Electronic Nose Drift Compensation Algorithm Based on Semi-Supervised Adversarial Domain Adaptive Convolutional Neural Network", *Sensors and Actuators B: Chemical*, Vol. 422, p. 136642, (2025).
- [4]. K. A. Alaghbari, H. S. Lim, M. H. M. Saad, and Y. S. Yong, "Deep Autoencoder-Based Integrated Model for Anomaly Detection and Efficient Feature Extraction in IoT Networks", *Internet of Things*, Vol. 4, No. 3, pp. 345–365, (2023).
- [5]. A. Mikhailova, N. M. Adams, C. A. Hallsworth, F. D. H. Lau, and D. N. Jones, "Unsupervised Deep-Learning-Powered Anomaly Detection for Instrumented Infrastructure", *Proceedings of the Institution of Civil Engineers – Smart Infrastructure and Construction*, Vol. 172, No. 4, pp. 135–147, (2020).
- [6]. W. Ni et al., "Multi-Task Deep Learning Model for Quantitative Volatile Organic Compounds Analysis by Feature Fusion of Electronic Nose Sensing", *Sensors and Actuators B: Chemical*, Vol. 417, (2024).
- [7]. J. Fonollosa, S. Sheik, R. Huerta, and S. Marco, "Reservoir Computing Compensates Slow Response of Chemosensor Arrays Exposed to Fast Varying Gas Concentrations in Continuous Monitoring", *Sensors and Actuators B: Chemical*, Vol. 215, pp. 618–629, (2015).
- [8]. X. Zhao et al., "Mixture Gases Classification Based on Multi-Label One-Dimensional Deep Convolutional Neural Network", *IEEE Access*, Vol. 7, pp. 12630–12637, (2019).
- [9]. S. Zhai, Z. Li, H. Zhang, L. Wang, S. Duan, and J. Yan, "A Multilevel Interleaved Group Attention-Based Convolutional Network for Gas Detection via an Electronic Nose System", *Engineering Applications of Artificial Intelligence*, Vol. 133, p. 108038, (2024).

TÓM TẮT

Phát hiện bất thường trong hỗn hợp khí sử dụng mảng cảm biến dựa trên học sâu không giám sát

Phát hiện bất thường trong dữ liệu hỗn hợp khí là một thách thức quan trọng đối với các hệ thống mảng cảm biến do tính phi tuyến, nhiễu, tác động của môi trường và sự thiếu hụt dữ liệu bất thường. Bài báo này đề xuất một phương pháp phát hiện bất thường dựa trên học sâu không giám sát. Mô hình Autoencoder được sử dụng để học đặc trưng biểu diễn ảnh hai chiều của dữ liệu hỗn hợp khí bình thường thông qua cơ chế tái tạo tín hiệu đầu vào mà không yêu cầu nhãn bất thường trong quá trình huấn luyện. Để mô phỏng các điều kiện bất thường thực tế, các mẫu bất thường được tạo ra bằng các biến đổi có ý nghĩa vật lý và đa dạng. Ngưỡng thích nghi dựa trên sai số tái tạo được sử dụng làm tiêu chí phân biệt giữa dữ liệu bình thường và bất thường. Hiệu quả của phương pháp được đánh giá thông qua các chỉ số accuracy là 0.97 và F1-score là 0.92. Kết quả thực nghiệm cho thấy phương pháp đề xuất có khả năng học hiệu quả đặc trưng của dữ liệu bình thường và phát hiện chính xác các bất thường trong dữ liệu hỗn hợp khí. Phương pháp này góp phần nâng cao độ an toàn, tin cậy và khả năng giám sát thông minh cho các hệ thống đa cảm biến khí trong các ứng dụng thực tế.

Từ khóa: Phát hiện bất thường; Học không giám sát; Autoencoder; Mảng cảm biến khí.